

Development of Improved Radiation Drive Environment for High Foot Implosions at the National Ignition Facility

D. E. Hinkel,¹ L. F. Berzak Hopkins,¹ T. Ma,¹ J. E. Ralph,¹ F. Albert,¹ L. R. Benedetti,¹ P. M. Celliers,¹ T. Döppner,¹ C. S. Goyon,¹ N. Izumi,¹ L. C. Jarrott,¹ S. F. Khan,¹ J. L. Kline,² A. L. Kritcher,¹ G. A. Kyrala,² S. R. Nagel,¹ A. E. Pak,¹ P. Patel,¹ M. D. Rosen,¹ J. R. Rygg,¹ M. B. Schneider,¹ D. P. Turnbull,³ C. B. Yeaman,¹ D. A. Callahan,¹ and O. A. Hurricane¹

¹Lawrence Livermore National Laboratory, Livermore, California 94550, USA

²Los Alamos National Laboratory, Los Alamos, New Mexico 87545, USA

³Laboratory for Laser Energetics, University of Rochester, Rochester, New York 14625, USA

(Received 10 June 2016; published 23 November 2016; corrected 13 February 2017)

Analyses of high foot implosions show that performance is limited by the radiation drive environment, i.e., the hohlraum. Reported here are significant improvements in the radiation environment, which result in an enhancement in implosion performance. Using a longer, larger case-to-capsule ratio hohlraum at lower gas fill density improves the symmetry control of a high foot implosion. Moreover, for the first time, these hohlraums produce reduced levels of hot electrons, generated by laser-plasma interactions, which are at levels comparable to near-vacuum hohlraums, and well within specifications. Further, there is a noteworthy increase in laser energy coupling to the hohlraum, and discrepancies with simulated radiation production are markedly reduced. At fixed laser energy, high foot implosions driven with this improved hohlraum have achieved a $1.4 \times$ increase in stagnation pressure, with an accompanying relative increase in fusion yield of 50% as compared to a reference experiment with the same laser energy.

DOI: 10.1103/PhysRevLett.117.225002

Recent high foot implosions [1] at the National Ignition Facility (NIF) [2] have demonstrated alpha heating, where a sufficiently compressed pellet of deuterium (D) and tritium (T) generates alpha particles that deposit energy back in to the central hot spot and amplify the neutron yield that is produced by compression alone. Analyses of this series of experiments [3,4] indicate that improvements in the radiation environment can significantly enhance implosion performance. Such improvements include more symmetric radiation drive, as seen by the DT pellet, as well as improved energy coupling from the laser to the radiation cavity, with a reduction in hot electrons (generated by parametric processes) that preheat the fuel. In this Letter, we describe how we achieved these improvements in the radiation environment and how implosions fielded with these improvements indeed show enhanced performance.

The process of indirectly driven laser fusion [5] uses a high-Z radiation cavity (i.e., a “hohlraum”) to convert laser energy to x-ray energy. The hohlraum must provide the necessary radiation drive for compression, and it must do so in a symmetric fashion. Suspended in the middle of the hohlraum is a capsule of DT encased in a plastic shell. Radiation generated by the hohlraum bathes the capsule, ablating material from its outside, and, through conservation of momentum, the capsule then implodes. Compression of the capsule with radiation forms a central “hot spot” where fusion occurs [$D + T \rightarrow \alpha(3.5 \text{ MeV}) + n(14.1 \text{ MeV})$]. With successful assembly of the hot spot,

the plasma ignites and the compressed fuel burns a small fraction ($<15\%$) of its mass as it disassembles.

Conventional hohlraums for high foot implosions, which are 5.75 mm in diameter and 9.3 mm in length [cf. Fig. 1(a)], are filled with He gas at a high gas fill density, 1.6 mg/cc. This high fill density tamps hohlraum wall motion during the laser pulse, which is $\sim 13\text{--}15$ ns in length.

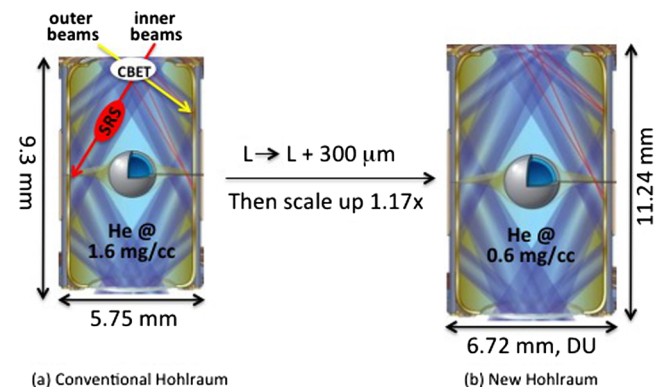


FIG. 1. (a) A conventional hohlraum for high foot implosions is filled with He gas at high density (1.6 mg/cc), through which the inner beams struggle to propagate. To compensate, we utilize CBET to transfer energy from outer to inner beams. SRS occurs along the inner beams, generates hot electrons, and exacerbates drive asymmetry. (b) The new hohlraum for high foot implosions is longer, larger, and fielded at lower gas fill density (0.6 mg/cc). This produces less SRS along the inner beams, and mitigates the need for CBET.

With this high gas fill density, the inner beams struggle to propagate to the wall for reasons that are not completely understood, and thus the capsule waist becomes radiation starved as compared to the pole, resulting in symmetry distortion in the Legendre P2 modes. In addition, laser backscatter [6] levels are high along the inner beams in these hohlraums, which serves to further starve the capsule waist of radiation drive. To compensate, we employ cross-beam energy transfer (CBET), where a wavelength difference on the order of 0–10 Å (at 1ω) between the outer and inner beams is used to transfer energy to the inners via a shared ion acoustic wave [7]. While CBET has been employed to drive implosions round (i.e., $|P2| \leq 4 \mu\text{m}$) it involves complexities described below. Additionally, these conventional hohlraums produce a Legendre P4 asymmetry because of their length and beam pointing, as discussed below.

To improve the radiation drive environment, we hypothesize the need for a longer, larger hohlraum at lower gas fill density (LLL). Increasing the length of the hohlraum has been shown previously to improve P4 asymmetry [8]. Moreover, a lower gas fill density should improve inner beam propagation, as less inverse bremsstrahlung absorption will occur along inner beam paths. Additionally, laser backscatter levels along the inner beams should be reduced as well, because the beams are propagating through hotter, less dense plasma. However, since a lower gas fill density results in an increased inward expansion of the hohlraum wall (wall motion of cool, dense plasma plus a hot underdense “gold bubble”), and the wall needs to stay out the path of the inner beams, we choose to increase the hohlraum size. A larger hohlraum (where the “case-to-capsule ratio”, $R_{\text{hohlraum}}/R_{\text{capsule}}$ increases) provides more space between the wall and capsule waist, allowing for improved inner beam propagation. These improvements are valid for any hohlraum wall material. In the experimental results detailed below, the LLL hohlraum wall composition was chosen to be gold-lined depleted uranium (DU), which provides 1.065 times more drive than a gold (Au) hohlraum at the same laser energy [9].

Low gas-fill density hohlraums have already been proven with shorter laser pulses (5–8 ns) that are optimal for a high-density carbon ablator (HDC) [10]. Such short pulses are a consequence of the $3 \times$ higher density of HDC relative to plastic (CH) ablaters [11]. Here, for the first time, improved hohlraums have been fielded for high foot implosions, where DT capsules are coated with a CH ablator material, and the laser pulse lengths are in the range of 12–15 ns. The challenge is to maintain the shaped high foot radiation drive on a plastic capsule in a symmetric fashion using pulses that are twice as long as for HDC. The longer pulse leads to more wall motion, which has the potential, as mentioned above, to interfere with late-time inner beam propagation.

A NIF hohlraum (cf. Fig. 1) is typically a cylinder with Au, Au-lined DU, or unlined DU walls. At each end of the hohlraum is a laser entrance hole (LEH) through each of

which 96 beams propagate. The laser beams strike the inside of the hohlraum wall, where conversion to x-ray energy occurs. In conventional hohlraums, radiographs of the in-flight implosion show Legendre mode P4 capsule asymmetry [8], which can be improved by increasing the hohlraum length by 300 μm and keeping the outer beam locations fixed relative to the end cap. This method increases the distance between the inner and outer beams and successfully reduces the in-flight P4 by over a factor of 2, to 2.6%. (The in-flight P4 is measured at the time when the capsule radius has radially converged to $r = 200 \mu\text{m}$, i.e., a factor of ~ 5 .)

In addition to the increased hohlraum length [cf. Fig. 1(b)], the overall hohlraum scale is increased by $1.17\times$, and the helium gas fill density is decreased from 1.6 to 0.6 mg/cc. These two changes improve inner beam propagation to the wall, which helps ensure balance of drive on the waist of the capsule vs the pole.

Previously, P2 symmetry was accomplished at NIF by invoking cross-beam energy transfer (CBET) [7]. In LLL hohlraums, we strive to reduce our reliance on CBET, as this can introduce spatiotemporal radiation drive asymmetry. CBET results in spatially nonuniform laser beam spots generated by the volumetric overlap of inner and outer beams at the LEH [12]. Further, simulation analyses show that CBET has a complicated temporal history—turning on in the early part of the pulse, as the LEH windows are blowing down, and then turning off. CBET then turns on again as the laser pulse rises to peak power [12]. It is also plausible that the CBET turns itself off once again later in the main power pulse [3], contributing to the problem of reduced inner beam propagation.

In conventional hohlraums, P2 symmetry is further compromised by large amounts of laser backscatter along the inner beams in the form of stimulated Raman scatter (SRS) [6], where laser light scatters off self-generated electron plasma waves. Use of an LLL hohlraum mitigates SRS on the inner beams (reduced to 5.4% from 12.1%), since these beams (with a long path to the wall) propagate through lower density plasma at higher electron temperature. In turn, this reduction in backscatter, coupled with the greater space over the capsule waist for inner beam propagation, improves inner beam propagation thus mitigating the reliance on CBET.

While SRS on the inner beams is reduced in the improved hohlraum, stimulated Brillouin scatter (SBS) [6], where laser light scatters off self-generated ion acoustic waves, somewhat increases along the outer beams, from 3.4% up to 5.0%. With more wall motion in the improved hohlraum, the outer beams have a longer path length through high- Z wall material, where ion Landau damping is low, and more SBS is generated.

We note that the measured backscatter in LLL hohlraums is now within NIF ignition requirements, and that it occurs in a more symmetric fashion. Namely, inner and outer beams have similar levels of backscatter (5.4% on the

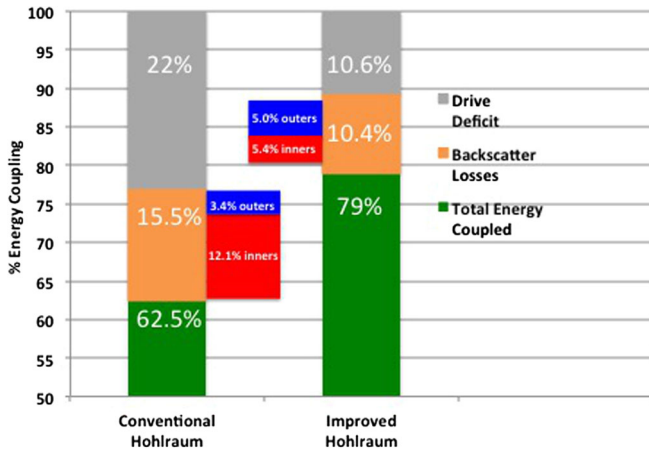


FIG. 2. An energy coupling summary for the improved hohlraum as compared to a conventional hohlraum. Overall energy coupling for the improved hohlraum is 79% as compared to 62.5% for the conventional hohlraum, with an error bar of $\sim +/ - 3\%$. Moreover, the measured backscatter, which has an error bar of $+/ - 20\%$ for high yield shots, is reduced and is more evenly distributed between inner and outer beams. The amount of energy not creating radiation drive, (drive deficit) is also reduced.

inners and 5.0% on the outers), whereas in the conventional hohlraum the bulk of the backscatter is on the inner beams (12.1% on the inners vs 3.4% on the outers).

Improvements in laser energy coupling to the hohlraum are summarized in Fig. 2. Analyses based on experimental results (i.e., bang time) and simulations (that match bang time) indicate that 62.5% of the incident laser energy creates radiation drive in the conventional hohlraum. The remainder of incident energy either exits the hohlraum as backscatter (15.5%), or does not create the radiation (22%) that the simulations expect to be produced, and thus is labeled as a “drive deficit” [13]. With the LLL hohlraum, 79% of the incident laser energy creates radiation, only 10.4% exits the hohlraum as backscatter, and the drive deficit has been reduced by over a factor of 2 from 22% to 10.6%. Multiple hypotheses for drive deficiency are detailed in Ref. [14], and this work eliminates those that invoke longer pulses as the cause. Research into drive deficiency is an ongoing effort, and the improvement reported here will serve as a test bed for furthering understanding, leading to even more efficient hohlraums. Interestingly, the $1.26 \times (= 79/62)$ improvement in radiation production in these LLL hohlraums compensates for the $1.3 \times$ increase in their wall area (and hence wall loss), resulting in similar drive to the conventional hohlraums, at the same incident laser energy, namely, a peak T_r of ~ 275 eV.

Hot electrons are created via laser-plasma interactions [6], and can be inferred from the bremsstrahlung generated when they interact with the hohlraum [15]. Figure 3 depicts the reduction in hot electron levels in the LLL hohlraum. A typical hot electron spectrum in a NIF hohlraum is best fit

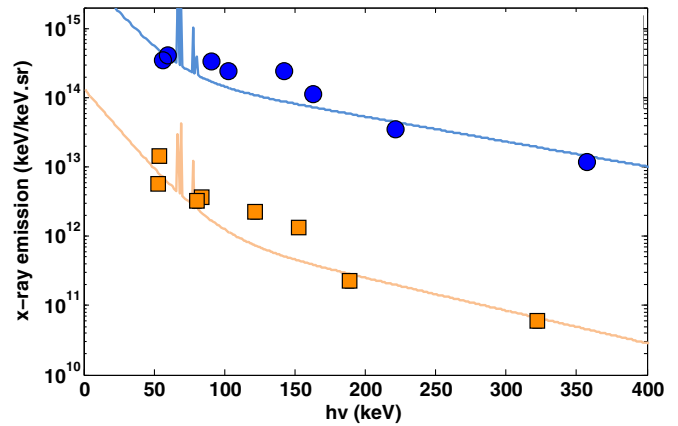


FIG. 3. A NIF hot electron spectrum fit by a two-temperature distribution. The temperature component at 18 keV is generated by SRS backscatter; at ~ 50 – 150 keV, by SRS forward scatter and two-plasmon decay. Hot electrons with energies > 170 keV prematurely heat the fuel, reducing target performance.

by a two-temperature distribution [15]. At a temperature of ~ 18 keV, hot electrons are generated by SRS backscatter [6]; at a temperature of ~ 50 – 150 keV, hot electrons are thought to be generated by SRS forward scatter and two-plasmon decay [6]. Sufficiently high numbers of hot electrons (> 180 J at energies above 170 keV [16]) can penetrate the capsule and prematurely heat the fuel, increasing its entropy, resulting in lower compression and reduced target performance. In the LLL hohlraum, the level of hot electron preheat is close to that of a near-vacuum hohlraum, which reported a $100 \times$ reduction from ~ 1 kJ to ~ 10 J [17].

The benefit of driving a high foot implosion with the radiation environment of an improved hohlraum was tested in a series of three shots, and the experimental results are summarized in Fig. 4. Shot N141106 (shown in blue) is a high foot implosion in a conventional hohlraum driven with a laser power and energy of 350 TW and 1.65 MJ, respectively. Using 230 kJ less energy in the improved hohlraum (Shot N151020, driven at 360 TW and 1.4 MJ, shown in purple) results in a neutron yield, fuel areal density (reported as a down-scattered ratio of neutrons, where $DSR = \text{fuel areal density}/20.3$) and low-mode (P2) hot spot x-ray self-emission symmetry at peak compression with substantial improvement. The primary neutron image also shows modest improvement to P2. Note that this P2 symmetry improvement occurs in the absence of CBET.

The best comparison of nuclear performance is N141106 vs N151111 (conventional hohlraum in blue vs improved hohlraum in red). These two implosions were driven at near-equal laser power and energy, after correcting for Au vs Au-lined DU equivalent energies, as described above. The neutron yield of N151111 is 1.5 times greater than that of N141106, and the total areal density (assembly of cold fuel + compressed shell around the central hot spot) is 1.2 times larger. This improvement in total areal density is

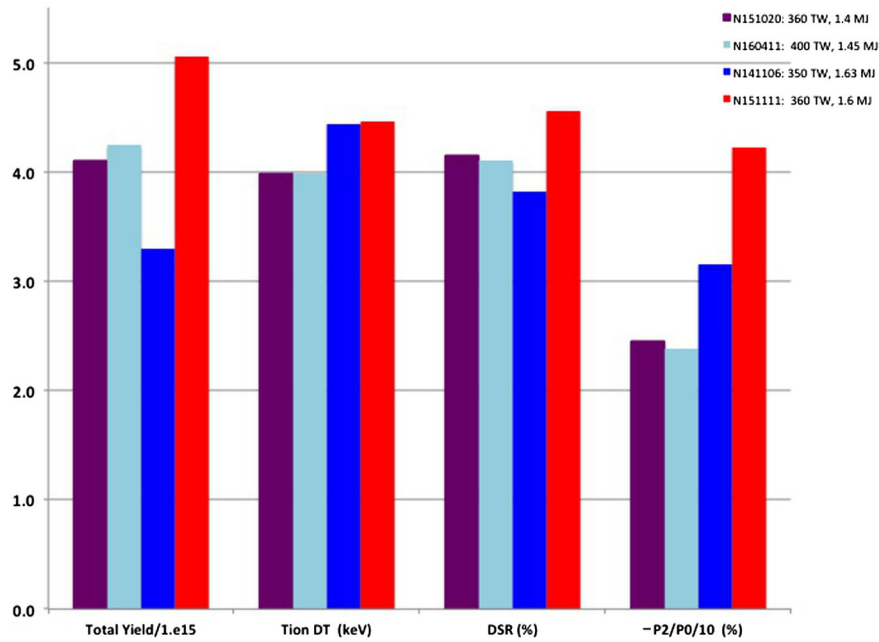


FIG. 4. Implosions driven with the improved hohlraum outperform those driven with a conventional hohlraum in the range of 350–400 TW peak power, and 1.4–1.65 MJ of laser energy. Blue implosion metrics are for a high foot implosion in a conventional hohlraum. Purple, red, and cyan depict the same metrics in the improved hohlraum. Error bars on total yield are $\pm 2.8\%$, whereas on DSR the error bar is $\pm 5 - 7.5\%$. The error bar on the Brysk Tion is $\pm 3 - 5\%$, and that for P2/P0 is $\pm 2 - 5\%$.

presumed to derive from a reduction in hot electrons and a slight decrease in first shock velocity, both of which reduce implosion entropy. Potential future experiments using this low hot electron radiation environment, but with a similar first shock velocity to that used in conventional hohlraums, would quantify their relative contributions. The central hot spot ion temperature is nearly equal for these two implosions. All three shots in the improved hohlraum have achieved a $\sim 1.4 \times$ improvement (to ~ 180 Gbar) in the inferred stagnation pressure, as calculated by the methodology of Ref. [1]. Interestingly, N151111 (no CBET) shows these substantial improvements even though the low-mode (P2) symmetry is degraded $\sim 1.33 \times$ compared to that of N141106 (substantial CBET). This suggests that symmetry swings, perhaps associated with CBET, are a source of performance degradation [18].

In an effort to improve P2 symmetry, we fielded implosion N160411 in the improved hohlraum at a laser power and energy of 400 TW and 1.45 MJ (i.e., an implosion comparable to N151020, but with a laser pulse that is shorter by 250 ps and at slightly higher laser power, but at the same laser energy. A small, $12 \times 4 \times 2 \mu\text{m}^3$ gold flake was present on the surface of the N160411 capsule at shot time—calculations indicate that this flake would have caused a hydrodynamic jet in to the hot spot, but it is not clear how this impacts net performance. As shown in cyan, the key metrics for N160411 are nearly equivalent to those for N151020 (purple). Shot N160411 does show improved symmetry, as described in the next paragraph.

Another improvement metric is the uniformity of capsule compression, or the level of primary neutron yield anisotropy as a function of angle, which is measured using

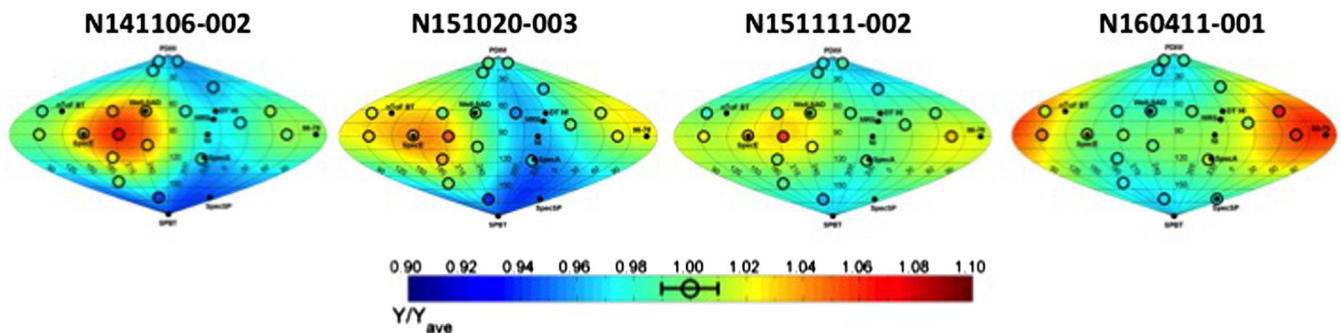


FIG. 5. Spatial plots of primary neutron yield from the nuclear activation diagnostic. Yield higher (lower) than average corresponds to thin (thick) spots in the assembled fuel. The improved hohlraum results in uniformity improvement by $1.2 - 1.7 \times$. Some nonuniformities may be due to engineering features (such as the capsule fill tube), which are not mitigated with this new hohlraum.

thick zirconium foils placed on the outside of nine diagnostic port covers around the chamber [19]. Figure 5 plots the primary neutron yield over the average for our suite of shots. Yield higher (lower) than average corresponds to thin (thick) spots in the assembled fuel. The images are depicted on a scale of 90%–110% of the average yield. Since the range of a 14.1 MeV neutron in DT is 5 gm/cm², a 10% yield deficit corresponds to 0.5 gm/cm² areal density variation. Detailed analyses of our data lead to a determination that use of this improved hohlraum results in an increase in capsule compression uniformity by 1.2–1.7×. Most notable is an improvement in polar thickness variations at the poles.

In summary, fielding high foot implosions in a longer, larger hohlraum at lower gas fill density has resulted in a significantly better hohlraum, which in turn provides a radiation environment that improves implosion performance. Future shots in this campaign include a further increase in laser power and energy as well as invoking a modest amount of CBET to improve P2 symmetry. Additionally, we plan to increase the ratio of hohlraum to capsule size, which should also improve P2 symmetry. Such modifications will enhance our scientific understanding of high foot, and other x-ray driven implosions and provide guidance along the path toward ignition.

The authors would like to thank the ICF Program Summer Study for the initial recommendation of fielding high foot implosions in improved hohlraums [20]. We also acknowledge the careful manuscript reading by O. L. Landen, whose suggestions improved this Letter. This work was performed under the auspices of the U.S. Department of Energy by Lawrence Livermore National Laboratory under Contract No. DE-AC52-07NA27344, Lawrence Livermore National Security, LLC.

-
- [1] O. A. Hurricane *et al.*, *Nature (London)* **506**, 343 (2014).
 [2] J. A. Paisner, E. M. Campbell, and W. J. Hogan, National Technical Information Service Documents No. DE95017671–DE95017673 and No. DE95017676–DE95017700; E. Moses, R. Boyd, B. Remington, C. Keane, and R. Al-Ayat, *Phys. Plasmas* **16**, 041006 (2009).
 [3] A. L. Kritcher *et al.*, *Phys. Plasmas* **23**, 052709 (2016).
 [4] D. S. Clark, C. R. Weber, J. L. Milovich, J. D. Salmonson, A. L. Kritcher, S. W. Haan, B. A. Hammel, D. E. Hinkel, O. A. Hurricane, O. S. Jones, M. M. Marinak, P. K. Patel, H. F. Robey, S. M. Sepke, and M. J. Edwards, *Phys. Plasmas* **23**, 056302 (2016).
 [5] J. D. Lindl, *Inertial Confinement Fusion* (Springer-Verlag, New York, 1998).
 [6] J. F. Drake, P. K. Kaw, Y. C. Lee, G. Schmidt, C. S. Liu, and M. N. Rosenbluth, *Phys. Fluids* **17**, 778 (1974); D. W. Forslund, J. M. Kindel, and E. L. Lindman, *Phys. Fluids* **18**, 1002 (1975); W. L. Kruer, *The Physics of Laser-Plasma Interactions*, Frontiers in Physics Series (Addison-Wesley, Redwood City, 1988), Vol. 73.
 [7] P. Michel, L. Divol, E. A. Williams, S. Weber, C. A. Thomas, D. A. Callahan, S. W. Haan, J. D. Salmonson, S. Dixit, D. E. Hinkel, M. J. Edwards, B. J. MacGowan, J. D. Lindl, S. H. Glenzer, and L. J. Suter, *Phys. Rev. Lett.* **102**, 025004 (2009).
 [8] J. R. Rygg, O. S. Jones, J. E. Field, M. A. Barrios, L. R. Benedetti, G. W. Collins, D. C. Eder, M. J. Edwards, J. L. Kline, J. J. Kroll, O. L. Landen, T. Ma, A. Pak, J. L. Peterson, K. Raman, R. P. J. Town, and D. K. Bradley, *Phys. Rev. Lett.* **112**, 195001 (2014).
 [9] T. Döppner *et al.*, *Phys. Rev. Lett.* **115**, 055001 (2015).
 [10] O. Jones, N. Izumi, L. B. Hopkins, D. J. Strozzi, P. A. Amendt, G. N. Hall, D. D. Ho, S. F. Khan, N. B. Meezan, J. D. Moody, S. R. Nagel, J. E. Ralph, and R. P. J. Town, *Bull. Am. Phys. Soc.* **59** (15), 66 (2014); P. Amendt, D. D. Ho, and O. S. Jones, *Phys. Plasmas* **22**, 040703 (2015); L. F. Berzak Hopkins, S. Le Pape, L. Divol, N. B. Meezan, A. J. Mackinnon, D. D. Ho, O. S. Jones, S. Khan, J. L. Milovich, J. S. Ross, P. Amendt, D. Casey, P. M. Celliers, A. Pak, J. L. Peterson, J. Ralph, and J. R. Rygg, *Phys. Plasmas* **22**, 056318 (2015); O. S. Jones, C. A. Thomas, P. A. Amendt, G. N. Hall, N. Izumi, M. A. Barrios Garcia, L. F. Berzak Hopkins, H. Chen, E. L. Dewald, D. E. Hinkel, A. L. Kritcher, M. M. Marinak, N. B. Meezan, J. L. Milovich, J. D. Moody, A. S. Moore, M. V. Patel, J. E. Ralph, S. P. Regan, M. D. Rosen, M. B. Schneider, S. M. Sepke, D. J. Strozzi, and D. P. Turnbull, *J. Phys. Conf. Ser.* **717**, 012026 (2016).
 [11] A. J. MacKinnon *et al.*, *Phys. Plasmas* **21**, 056318 (2014).
 [12] L. A. Pickworth, M. B. Schneider, D. E. Hinkel, M. D. Rosen, F. Albert, D. A. Callahan, P. A. Michel, A. E. Pak, E. A. Williams, J. D. Moody, S. S. Wu, L. R. Benedetti, and A. Moore, *Proceedings of the 56th Annual Meeting of the APS Division of Plasma Physics*, [http://meetings.aps.org/link/BAPS.2014.DPP.CO4.10.](http://meetings.aps.org/link/BAPS.2014.DPP.CO4.10.;); E. L. Dewald, J. Milovich, C. Thomas, J. Kline, C. Sorce, S. Glenn, and O. L. Landen, *Phys. Plasmas* **18**, 092703 (2011).
 [13] O. S. Jones *et al.*, *Phys. Plasmas* **19**, 056315 (2012).
 [14] M. D. Rosen, H. Scott, D. Callahan, D. Hinkel, P. Amendt, and L. Berzak Hopkins, *Proceedings of the 41st EPS Conference on Plasma Physics Paper O2.206*. On line Europhysics Conference, Vol **38F**, ISBN-2-914771-90-8, <http://ocs.ciemat.es/EPS2014PAP/pdf/O2.206.pdf>.
 [15] M. Hohenberger, F. Albert, N. E. Palmer, J. J. Lee, T. Döppner, L. Divol, E. L. Dewald, B. Bachmann, A. G. MacPhee, G. LaCaille, D. K. Bradley, and C. Stoeckl, *Rev. Sci. Instrum.* **85**, 11D501 (2014).
 [16] S. W. Haan *et al.*, *Phys. Plasmas* **18**, 051001 (2011).
 [17] L. F. Berzak Hopkins *et al.*, *Phys. Rev. Lett.* **114**, 175001 (2015).
 [18] A. L. Kritcher, R. Town, D. Bradley, D. Clark, B. Spears, O. Jones, S. Haan, P. T. Springer, J. Lindl, R. H. H. Scott, D. Callahan, M. J. Edwards, and O. L. Landen, *Phys. Plasmas* **21**, 042708 (2014).
 [19] D. L. Bleuel *et al.*, *Rev. Sci. Instrum.* **83**, 10D313 (2012); C. B. Yeamans, D. L. Bleuel, and L. A. Bernstein, *Rev. Sci. Instrum.* **83**, 10D315 (2012); J. D. Lindl, *Inertial Confinement Fusion* (Springer-Verlag, New York, 1998), Chap. 11.
 [20] Report on the August 2014 National Ignition Facility Data Review, Report No. LLNL-AR-666385, edited by M. D. Rosen and J. Edwards.